POLITECNICO DI TORINO

SCUOLA INTERPOLITECNICA DI DOTTORATO

Doctoral Program in Electronic Devices

Final Dissertation

Label-free photonic crystal technology for immunosensing applications

Davide Zecca

Tutor
prof. Fabrizio C. Pirri

Co-Tutors
dr. Tiziana Stomeo
prof. Thomas F. Krauss
prof. Massimo De Vittorio

Co-ordinator of the Research Doctorate Course
prof. Giovanni Ghione

04th April 2016

Abstract

The continue request in medical field of methods for the diagnosing and the monitoring of diffuse pathologies like cancer, Alzheimer and muscular dystrophy, has pushed the scientific research to focus its interest in the design of biosensors for fast and in-situ assays. Although several typology of biosensors has been proposed, label-free immunosensors are good candidates in the biomarkers detection thanks to a high bio-selective recognition and a simple read-out.

This thesis presents the research activity about the design, fabrication and testing of an immunosensor based on a Si_3N_4 2-D photonic crystal (PhC) in membrane configuration and further optimizations of the fabrication process of PhC membranes for biosensing applications.

The structure has been optimized by means of the finite difference time domain method (FDTD) in order to achieve peaks of reflectivity in the visible-near infrared spectrum. Subsequently, a nano-fabrication protocol exploiting e-beam lithography and dry/wet etching has been optimized, obtaining high resolution structures. Finally, the immunosensor has been functionalized with a layer of antibodies for the detection of the IL-6 protein and experimental tests has been performed, achieving a sensitivity of 1.5 pg/ml. A further step has been the optimization of the fabrication processes of PhC membranes for biosensing applications and their transferring from rigid substrate to flexible polymeric layer in order to achieve high integrable and biocompatible devices.

Acknowledgements

Lists of Papers

Paper I

D. Zecca, A. Qualtieri, G. Magno, M. Grande, V. Petruzzelli, B. Prieto-Simon, A. D'Orazio, M. De Vittorio, N.H. Voelcker, T. Stomeo, "Photonic crystal based immunosensor for clinical diagnosis", Photonics Conference, 2014 Third Mediterranean, 1–3 (2014). doi:10.1109/MePhoCo.2014.6866459

Paper II

D. Zecca, A. Qualtieri, T. Stomeo, M. De Vittorio, G. Magno, M. Grande, V. Petruzzelli, A. D'Orazio, B. Prieto-Simon, N.H. Voelcker, "2D photonic crystal membranes for optical biosensors", Photonics Technologies, 2014 Fotonica AEIT Italian Conference on, 1–3 (2014). doi:10.1109/Fotonica.2014.6843901

Paper III

D. Zecca, A. Qualtieri, G. Magno, M. Grande, V. Petruzzelli, B. Prieto-Simon, A. D'Orazio, M. De Vittorio, N.H. Voelcker, T. Stomeo, "Label-free Si_3N_4 photonic crystal based immunosensors for diagnostic applications", Photonics Journal, IEEE vol. 6, issue 6 (2014). doi: 10.1109/JPHOT.2014.2352625

Contents

Chapter 1

Introduction and motivations

1.1 Needs of innovative biosensors for biomarkers detection

In the last years, scientific research has been characterized by a massive effort into the design of devices and techniques for applications in fields like healthcare, environmental safeguard and food safety with the aim of the global improvement of the quality of life. In particular, the ageing of the society and the socio-economic burden faced each years by the governments in the healthcare sector have pushed medical research activities to focus their attention at the study of methods of advanced diagnosis and faster and cheaper monitoring than the actual laboratory procedures. These needs and the recent progress in nano and micro fabrication techniques have brought the spread of innovative point-of-care platforms called biosensors[1], providing high sensitivity and selectivity in the revelations and monitoring of biological and chemical compounds by means of portable instrumentation for in-situ assays.

A biosensor is a sensor able to detect the presence and the concentration of biological or chemical species, called analyte, in a particular environment, like gases or solutions, and to transform the detection event in measurable signals. Its general structure can be described as the union of two main blocks[2]–[4] (Figure1.1):

- **Biorecognition element** (also called **bioreceptor**): it is usually represented by chemical or biological material like cells, molecules, antibodies and proteins. Its task is to react with the species that has to be detected in a selective way, recognising the presence of the analyte without modifying it.

- **Transducer**: it transforms the biological or chemical signal derived from the reaction of the bioreceptor in a signal that can be revealed and measured. It can be electrochemical, optical, piezoelectric or thermic depending on the type of biorecognition block used.
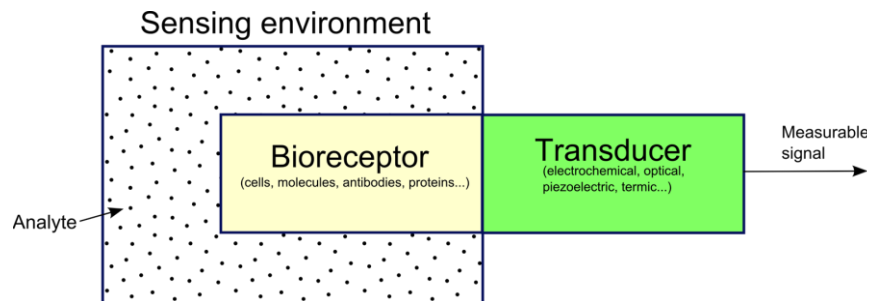
Figure 1.1: Block diagram of the components of a generic biosensor.

The different typologies of biosensors can be defined by the bioreceptor or the transducer used, starting the rise of a wide gamma of devices with different performances and suitable for various applications. Among these typologies there are the immunosensors[5],[6], that gather systems exploiting antibodies for a bio-specific recognition. As it is known, antibodies are the fundamental part of the immune system for recognising and destroying pathogenic agents. Each type of antibody binds only with another specific antigen. This feature and the possibility to synthesize antibodies in laboratory for any type of antigen[7] make them really appealing to be used as biorecognition elements for a wide variety of bio-chemical compounds, and in special way for biomarkers associated with pathological conditions.

A biomarker[8], [9] is a parameter containing important information about the states of a biological system and its processes, proving to be a valid instrument to diagnose diseases in subclinical manifestation, to follow their development and the reaction to drug treatments. Therefore, it is evident that the use of devices to monitor biomarkers in patients at risk and in the evaluation of the efficiency of a treatment it is essential to circumventing long waiting times and expensive

clinical assays. For these reasons, it is important to combine the antibodies detection with a transduction method which has to be efficient, with high sensitivity and not complex to be integrate. A possible solution is to use immunosensors based on optical read-out.

Optical read-out[6] include all the transduction methods using radiations to transform the biorecognition events in measurable signals. In literature, they can be divided in two groups:

- **Fluorescent based methods:** in this group there are techniques using fluorescent or radiative labels for the detection of the analyte in solution. Analytes are previously labelled with luminescent tags using chemical procedures. The sample is then measured, and the presence and concentration of the analyte are determinate by the quantity of radiation collected.
- **Label-free methods:** in this case the labelling step is not necessary because these are techniques based on the modification of the optical properties of a material or a structure due to the analyte.

Although fluorescent methods allow to reveal lower concentration of analyte than label-free ones, they need the sample preparation in laboratory, extending the assay time and not permitting in-situ analysis. Label-free biosensors[10] based on transduction methods like plasmonic[11]–[13], ring resonator[14], [15], waveguide[16], and whispering gallery mode[17] have been proposed in literature. Between these, photonic crystals (PhCs) based methods have been an important role[18]–[21], thanks their tunable electromagnetic properties and the high sensitivity to environmental parameters variations.

1.2 Work presented in this thesis

In this thesis the proof-of concept of a label-free immunosensor based on a 2-D photonic crystal slab for the revelation of biomarkers in solution is presented. The operation of the device is based on the detection of variations in the background refractive index: when the refractive index changes this variation is revealed by the structure with a change in the wavelength of the resonant peak. In this case, the refractive index change is due to the binding of the analyte on its surface, then associating the width of the peak shift with the amount of analyte, it is possible to have a quantitative assays. The structure has been functionalized with antibodies for the revelation of the interleukin-6 (IL-6)[22]–[24] protein, and experimental data have been collected in order to test the good operation of the sensor (results published in paper III).

The activities have been carried out within the frame work of the project entitled "Photonic Crystal Biosensors for Cardiac Biomarker Detection" funded by the Regione Puglia-South Australia Research Collaboration Award and have been divided between the three institutions as follows: the design and the preliminary experimental tests of the device have been carried out at the Politecnino di Bari; the IIT-CBN has dealt with the optimization of the fabrication protocol and the morphological characterization; finally, the functionalization of the immunosensor and the tests for the revelation of the IL-6 protein in solution has been performed at the Mawson Institute (University of South Australia).

The content of the thesis is divided as following: the next chapter deals with the optical properties of a 2-D photonic crystal slab, presenting the results of the numerical optimization of the structure used for the immunosensor. The third chapter illustrates the nano-fabrication protocol, highlighting the important parameters of each step. The last chapter (chapter 4) describes the functionalization and the experimental tests of the immunosensor in the detection of the IL-6 protein. The chapter is concluded with the activity realized

at the University of York, regarding the optimization of the fabrication process of suspended membranes for biosensing applications and the transferring of structures from rigid substrate to flexible polymeric layers, thus opening the way to a new generation of nanofabricated devices characterized by high resolution, integration and biocompatibility.

<div align="right">

Chapter 2

Design of the 2-D photonic crystal membrane for biosensing applications

</div>

2.1 Introduction

As it has been discussed in chapter 1, the optical read-out method represents one of the most promising mechanism for the realization of high sensitive sensors for medical and biochemical applications. In this field a particular attention is posed to the label-free immunosensors that, in contrast with the fluorescent read-out based sensors, do not need a preliminary labelling of the analyte with fluorescent probes, speeding up the assay procedure and avoiding contamination of the examined sample. A special role is covered by the label-free immunosensors exploiting photonic crystal structures as sensing block, that, thanks to their high sensibility to environmental variations, have been widely employed for the designing of new optical biosensors.

In the first part of the chapter the designed immunosensor will be presented, examining the electromagnetic behaviour of the 2-D photonic crystal slab, while the last part will illustrate the results related to the optimization of the geometrical parameters of the photonic crystal by means of the finite difference time domain (FDTD) method.

2.2 2-D photonic crystal slab and optical properties

Photonic crystals (PhCs) are structures that present a periodic profile of the refractive index in 1-D, 2-D or 3-D. By means of an appropriate choice of materials and geometrical parameters, it is possible to control the photons flowing into them. The interest in PhCs began in 1987 thanks to the studies carried on by Eli Yablonovitch[25] and Sajeev John[26], who proved the presence of a photonic

band gap[27] in the dispersion diagram of materials characterized by a 3-D periodic refractive index. Even if the presence of a photonic band gap in 1-D periodic structures was already discovered by Lord Rayleight in 1887[28], nobody before Yablonovitch and John had ever thought to extent the concept to 2-D and 3-D structures (Figure 2.1).
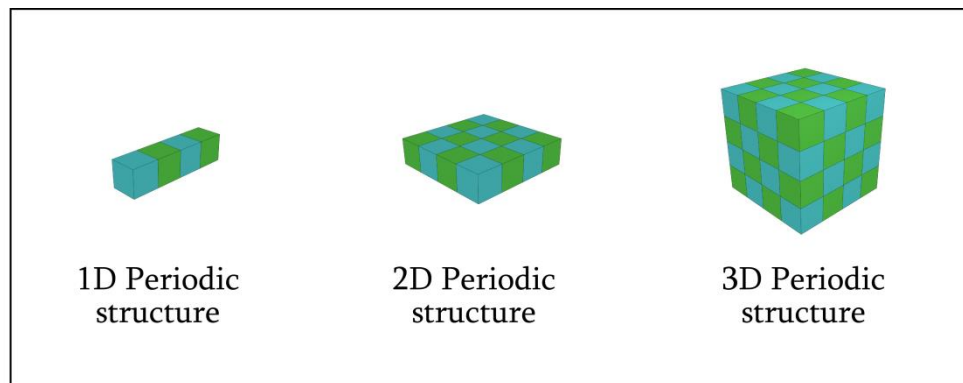
Figure 2.1: Sketches of structures with periodicity in 1-D, 2-D and 3-D. The two colours represent two materials with different refractive index.

Although at the beginning they were thought as optoelectronic components for telecommunications, through the time PhCs have also found wide application as sensing platform for chemical and biological sensors.

The sensor proposed in this thesis is a square lattice PhC patterned on a membrane of Si_3N_4 with area of 1 mm × 1 mm on a silicon (Si) substrate (Figure 2.2). The surface and the holes side-walls are covered with a uniform layer of antibodies with the aim to favour a bio-selective detection of the analyte of interest. When the analyte bound on the sensors, its presence causes a change in the surrounding refractive index producing a shift of the reflection peak. As discussed by El Beheiry et al.[29], the use of a 2-D PhC slab instead of other structural configurations brings some advantages as high sensitivity and simple coupling of the incident light beam. The reasons of this can be found in the optical properties of the slab.
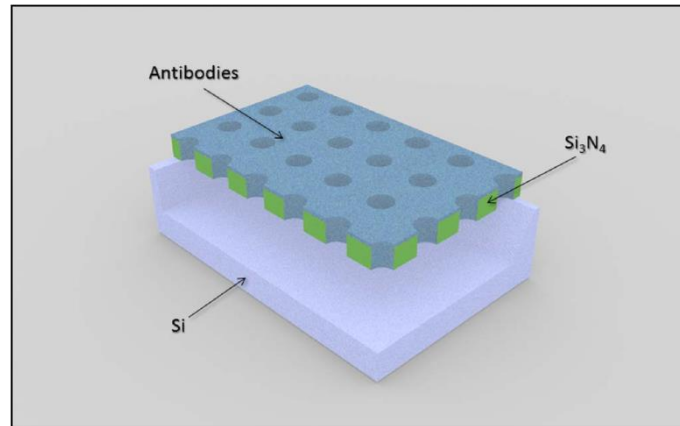
Figure 2.2: 3D model of the immunosensor.

In Figure 2.3 is represented the typical example of a fabricated 2-D PhC slab, which is constituted by a suspended membrane of material with high refraction index and finite thickness where the PhC is patterned. In this case two different mechanisms permit the propagation and the confinement of the light inside the structure: the radiation is confined in the x-y plane by means of a periodic disposition of the refractive index, while along z by means of the total internal reflection (TIR) due to the different refractive index of the slab and the background medium.
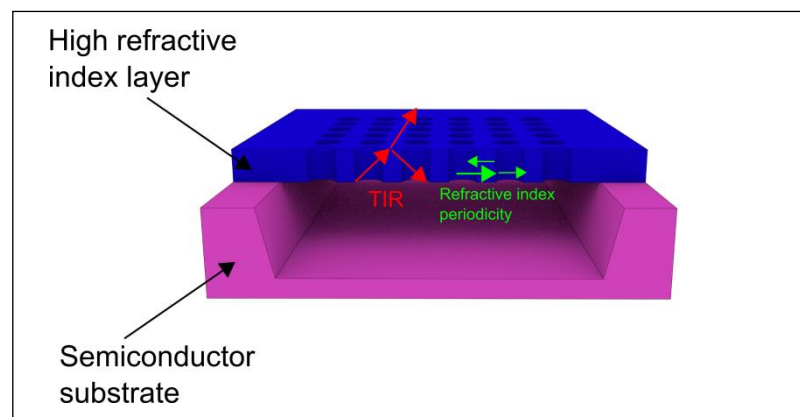
Figure 2.3: Section of a 2-D PhC slab representing the two different mechanisms that confine and propagate the radiation inside the structure: the TIR confines the radiation in the vertical direction, while the periodic disposition of the refractive index allows the flow in the planar direction.

Although a slab is able to approximate the electromagnetic characteristics of an ideal 2-D PhC, the not completely confined field takes relevant changes in the dispersion diagram. Because outside the slab the material is uniform and there are not changing in the refractive index, it is not possible to speak about bands and, in the same way, the lack of symmetry makes not possible the classification in TE and TM modes. This generates a continuum of states propagating in the free space called **light cone**[30] and represented by means of the blue zone in Figure 2.4. The width of the cone is related to the difference of refractive index between the slab and the background: higher is the difference, stronger will be the vertical confinement by means of the index guiding with a consequence reduction of the dispersion of radiation and the shrinking of the cone.
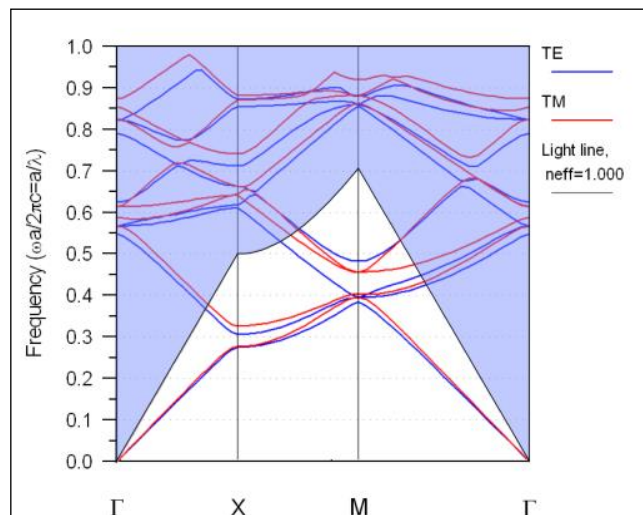
Figure 2.4: Typical dispersion diagram of a structure with finite height where the blue zone represents the dispersion of radiation in the surrounding medium.

Under the cone, the modes that are confined in the structures are subdivided in TE and TM and it is still possible to speak about a band gap even if it is no more complete like in the infinite z case because it is closed at the two ends by the continuum of the radiated states. In this case two type of guided modes can be supported called guided modes and resonant modes[31]: the first

ones are below the light line and are confined in the slab. The second one are the modes above the light cone, which are still confined in the slab but they can interact with the external environment. Sending an incident wave with normal direction to the slab, the interaction between the radiation and the resonant modes generates peaks in the transmission and reflection spectrums called Fano resonances[32]. These waveforms are very narrow and allow to sense very small variations in the parameters of the structure like changing in the surrounding refractive index.

Finally, the use of a membrane instead of a PhC cavity permits to collect signal from all the structure and to perform measurements with not complex or expansive equipment. In fact, although sensors exploiting cavities present higher sensitivity, the drawback of these devices is that their sensing area is mainly restricted at the cavity itself, where most of the electromagnetic field is located. Moreover, the measurements need the use of complex set-up able to focus the light beam in a small spot in the cavity, increasing the cost and making hard to integrate the devices in portable systems.

2.3 Design of the label-free immunosensor

The design and the simulation of the structure have been performed by the NanoPhotonics and Electromagnetics Group, (Dipartimento di Elettrotecnica ed Elettronica, Politecnico di Bari). The first step has been the choice of the material, that will influence the performance of the device and its fabrication process. In this case, the Si_3N_4 turns out to be the suitable material because it is transparent in the visible range and mechanically adequate for the large area membrane fabrication. Moreover, its refractive index (n ~ 2.0) guarantees a strong confinement of light in the structure while its biocompatibility avoids contamination in the biological measurements. The geometrical parameters of the PhC have been tuned to get peaks of the reflectivity spectrum in VIS-NIR range.

This has been done by systematic simulations of the structure, varying geometrical parameters like period and radius.

Even if the confinement in the vertical direction is regulated by the difference of refractive index at the interface, an important role is also played by the thickness of the membrane. As proposed by Johnson et al.[30], a good choice is to set the thickness to half the gap-bottom wavelength. In fact, if the membrane is too thin the modes are not well confined inside the slab and they are dispersed in the surrounding medium, at the contrary a thick slab permits the creation of higher-order modes in the band gap that can close the gap. In this case it has been chosen to hold the thickness fixed to 300 nm, getting a good trade out between mechanical properties of the membrane and sensing performances, avoiding the bowing and possible structural collapsing of the structure.

The software employed for the optimization is the Meep code[33], a free package for the FDTD simulation developed at MIT. The FDTD is a numerical method based on the Yee's algorithm[34] and used to simulate the behaviour of an electromagnetic field inside a region of space or a structure in a range of frequencies. It is based on the concept that making a discretization of the computational domain in a grid of cells, and arranging the components of the magnetic and electric field of each cell to obtain boundary condition involving perfectly conductive surfaces between the cells, it is possible to resolve an electromagnetic problem by means of the calculation in time and space of the Maxwell's curl-equations in a finite-difference approximations.

In Figure 2.5 it is represented the model used in the simulations: thanks to the symmetry in x and y directions presented in the PhC structure, it has been possible to simulate only an elementary cell and to use the periodic boundary conditions (PBC)[35] to repeat it in x and y directions. This has permitted to reduce sensibly the computational load and simulation time.
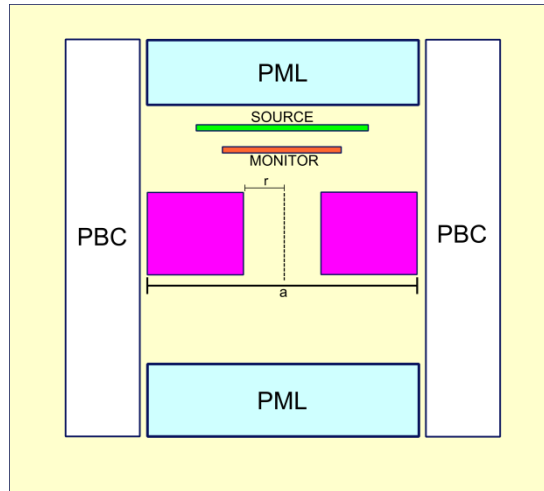
Figure 2.5: Model used in the FDTD optimization of the structure representing the unit cell of the PhC.

The cell is composed by a square slab with side of length *a*, thickness *t* and length of refractive index n_{Si3N4}=2.0 immersed in phosphate buffer solution, which is commonly used in chemical assays with refractive index n_{PBS}=1.34. The hole has radius *r* and is filled with the same material of the background. The structure has been excited by means of a wide range gaussian type source and centred in the wavelength of interest (λ_0 = 633 nm), while the reflected radiation has been collected by a monitor placed below the source.

A further condition to take into account in the use of the FDTD for PhCs simulations regards the imposition of absorption conditions on the boundaries of the computational domain that are not defined in its standard formulation. In fact, the radiation reaching the boundaries is partially reflected and partially transmitted, instead the simulation of PhCs requires the radiation arriving on the limits has to be completely transmitted. The perfectly matched layer (PML) condition is the most diffuse method to truncate the computational domain and it is based on the creation of an artificial material completely absorbent placed on the limit of the domain characterized by an increasing conductibility in function of the distance from the boundaries. In this case, a PML material has been used to avoid unwanted reflections at the edges of the domain along the z axis.

In Figure 2.6 are reported a series of simulations for different periods and

radius and their respective reflectivity maps. Based on these results, we decide to
concentrate the attention on a period p = 460 nm and radius r = 0.25*p (Figure
2.7a). For this structure measurements of sensitivity have been made by changing
the refractive index of the background material getting a value of 320 nm/RIU
(Figure 2.7b).
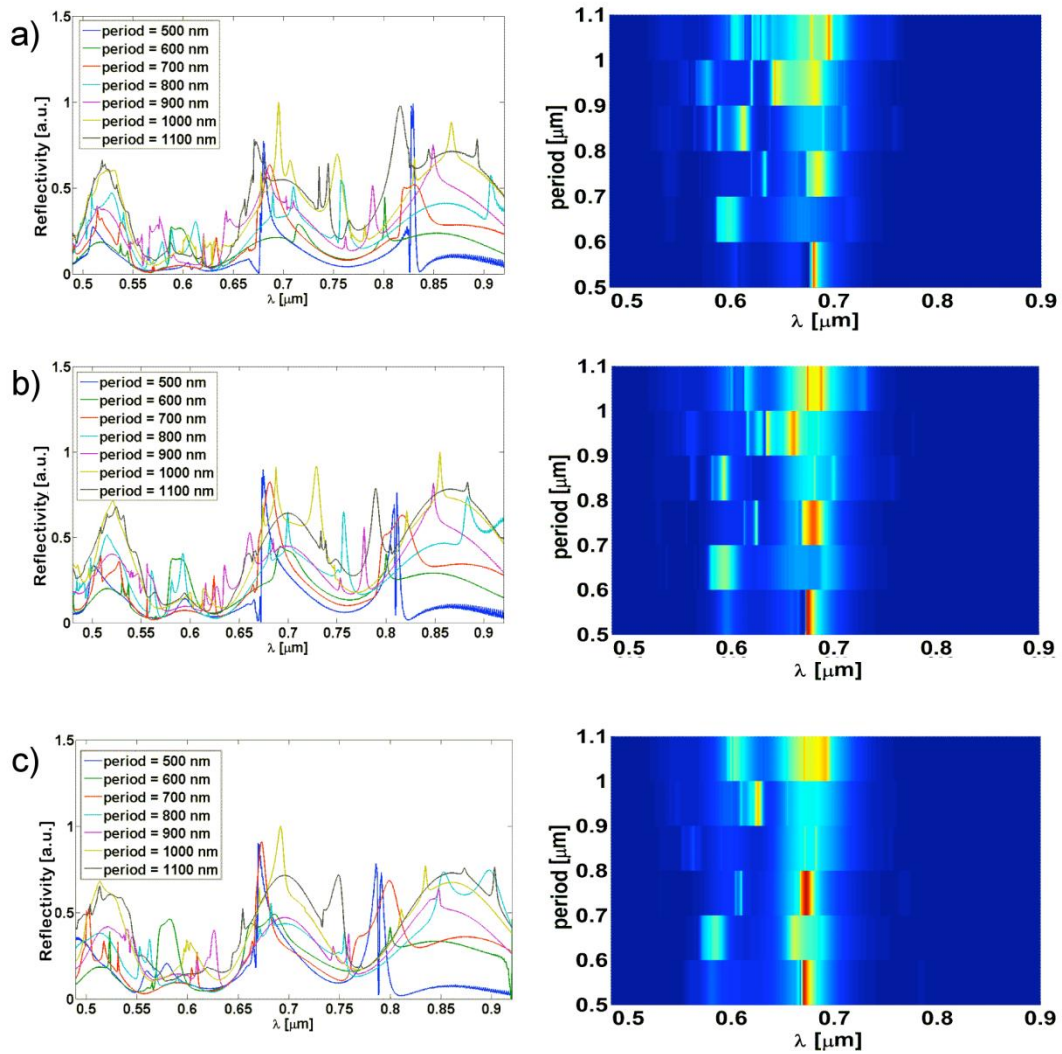
Figure 2.6: FDTD simulations and reflectivity spectrums of structures with different radius and period performed in PBS
environment: a) r = 0.25*p; b) r = 0.3*p; r = 0.35*p.
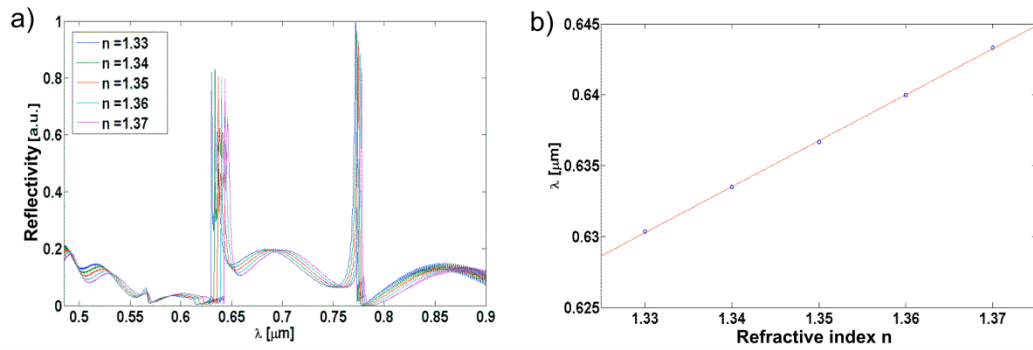
Figure 2.7: Sensitivity simulations for the PhC with (p = 460 nm r = 0.25*p): a) Reflectivity spectrums for different background refractive indexes; b) Shift of the 1st peak of reflectivity.

2.4 Summary

In this chapter the structure used as sensing block for the immunosensor has been presented, describing its optical properties and the advantage to use a 2-D PhC slab instead of another configuration. Finally, the structure has been simulated using the FDTD method, defining the geometrical parameters of the PhC. The next chapter will deal with the nano-fabrication protocol used to realize the device, describing the used technics and the achieved results.

Chapter 3

Fabrication of the 2-D photonic crystal membrane

3.1 Introduction

The fabrication of photonic crystals structures is a complex process that needs the use of advanced techniques in order to achieve reproducible nanoscale patterns with high resolution, making the choice of the fabrication steps and their set up a crucial point.

In this chapter will be explained the process used to fabricate the 2-D photonic crystal (PhC) structure in membrane configuration used as sensing block for the immunosensor. The process it is composed by the following steps:

1. electron beam lithography (EBL) to define the PhC pattern on a resist layer deposited on the sample by spin-coating;

2. dry etching of the Si_3N_4 by inductively plasma etching (ICP) using the patterned resist as mask;

3. wet etching by tetramethylammonium hydroxide (TMAH) solution to release the PhC membrane by removing the silicon underneath.

3.2 Fabrication process

Once the designing parameters have been established (paragraph 2.3), the device has been fabricated entirely in the facilities of the IIT-CBN centre, which has state-of-the-art fabrication facilities for the production of integrated photonic devices. The fabrication of PhC structures is a procedure requiring to achieve nanoscale structures with high resolution and, for these reasons, the choice of the adequate fabrication technologies is a key point to obtain high quality and

reproducible structures. The wafer used consisted of a double side of Si_3N_4 (thickness 300 nm) on Si substrate (thickness 440 μm). The fabrication protocol is reported in Figure 3.1 and it is mainly composed by electron beam lithography (EBL), inductively coupled plasma etching (ICP) and tetramethylammonium hydroxide (TMAH) wet etching for the membranes releasing.
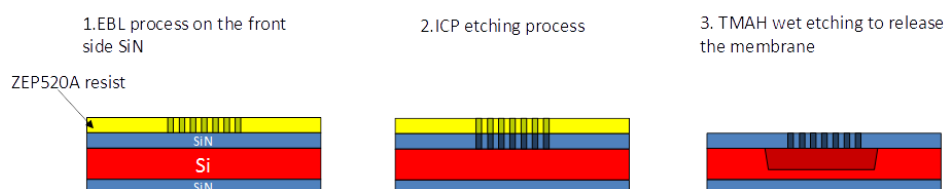
Figure 3.1: Fabrication process of the immunosensor.

3.3 Electron beam lithography (EBL)

The electron beam lithography (EBL) allows to impress the pattern directly on the resist without the use of masks, achieving results characterized by higher resolution and diffraction-limit than other optical methods[36]. For these reasons, it has been widely used for PhCs fabrication[37],[38] where resolution at nanoscale is the relevant point. These properties are due to the use of an electronic beam to expose the resist (Figure 3.2), avoiding the diffraction limit issue of the optical lithographic systems. The focused electron beam is generated inside the column by means of the extraction of electrons from a metallic filament, called cathode. Then, an anode accelerates the electrons along the column with energies of keV applied on it, while a series of electromagnetic lenses are used to focus and collimate the beam and to correct optical defects like astigmatism and aberrations.

Figure 3.2: Schematic of an EBL system.

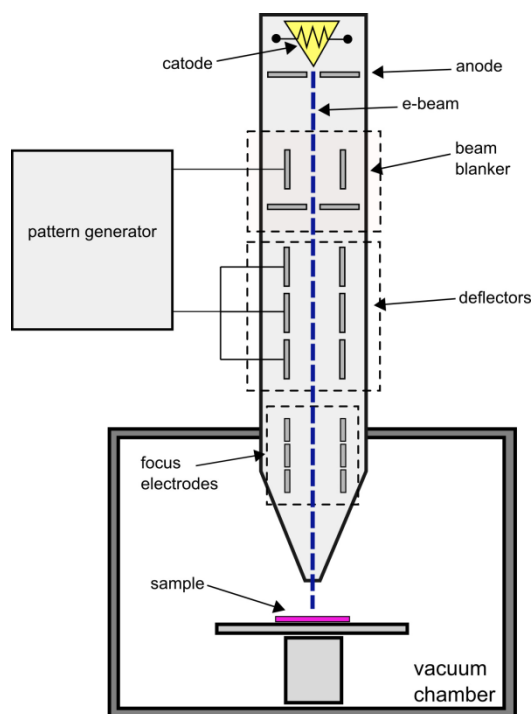The geometries that have to be transferred on the resist are contained in a CAD file that the operator edits and loads in the machine software before running the process. The information included in this file are used by the pattern generator to deflect the beam in the scan region by means of a series of electrodes to whom is applied a variable voltage. In the case of the immunosensor the pattern was represented by a 1 mm × 1mm PhC structure that it is subsequently released by wet etching to achieve a free-standing structure. Although the using of the Si_3N_4 guarantees optimal mechanical properties, the large area of the membrane can introduce stress in the structure with consequent losses in optical performance. Then, it has been designed a pattern that reproduces the same optical properties of a large area PhC membrane but more robust. As showed in Figure 3.3, it is composed by a 10 × 10 matrix of 100 μm × 100 μm membranes, providing a resistant device with a large sensing area. The distance between each membrane does not influence the electromagnetic behaviour of the entire structure because it is less of 10% of all the area.

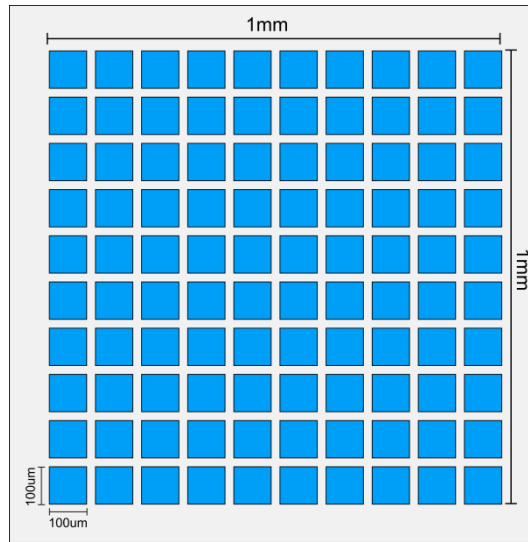**Figure 3.3:** Pattern written during the EBL process. Each blue square is a membrane of 100 μm×100 μm arranged in a 10 × 10 matrix, in order to obtain a total membrane 1 mm × 1 mm large.

Figure 3.4: RAITH150 at the IIT-CBN in Lecce (Italy).

The EBL has been performed with a RAITH150 (Figure 3.4) system using the following parameters:

- Acceleration voltage: 20 kV

- Aperture: 7.5 um

- Area dose: 50 $\mu C/cm^2$

- Dose factor: 1.2

- Step size: 0.01 μm

Even if the EBL shows small-diffraction limit, it is affected by a phenomena, called **proximity effect**[39], responsible in the reduction of the quality of the process: like in optical lithography the diffraction at micrometric scale leads to obtain structures with larger dimensions, in the case of EBL the interactions of the electrons with resist and substrate creates scattering effects when the beam goes through them, enlarging the incident beam diameter and bringing electrons to impress areas that can be several microns far from the exposure area (Figure 3.5). This effect has not a high influence for micrometric fabrication, but it becomes really relevant for dense nanometric pattern like PhCs.

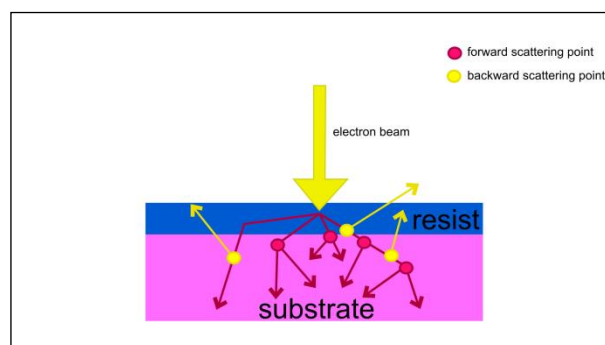**Figure 3.5:** Sketch reproducing the two scattering phenomena occurring when the electrons of the beam interact with the atomic structure of the resist and the substrate.

Even if these scattering events are intrinsic of the process, it is possible to contrast them modifying the pattern dimensions or the dose distribution. In the case of the 2-D PhC used for the immunosensor, the fastest solution to avoid the

widening of the features has been to keep the dose fixed and to reduce the dimensions of the holes in the pattern of a quantity equal to the enlargement factor but, for complex structures, the proximity effect correction is achieved by means of more elaborated numerical methods, where the computational complexity increases with the desired accuracy[40]–[42].

Finally, the EBL process is also strictly related to the choice of the electronic resist and the design of the pattern that has to be impressed on it. In this case the resist used is the ZEP520A that, in addition to its high resolution, presents a strong resistance for the use as mask for the ICP dry etching[43].

The deposition has been done by means of spin coating with spin speed based on the wanted thickness. In this process the resist thickness has been of 400 nm, ensuring both a resistance at the dry etching and a good resolution for the EBL process. The optimized parameters used were:

- spin speed 2500 rpm for 40 s
- post baked for 10 minutes at 180°C

After the lithography the sample has been rinsed in the xylene developer solution at 23°C for 45s removing all the exposed resist. Figure 3.6 shows a cross section acquired by scanning electron microscopy (SEM) of the high quality 2D-PhC pattern achieved into the ZEP520A e-beam resist after the development. A platinum (Pt) layer has been deposited on the pattern in order to protect the structure during the FIB cross section.
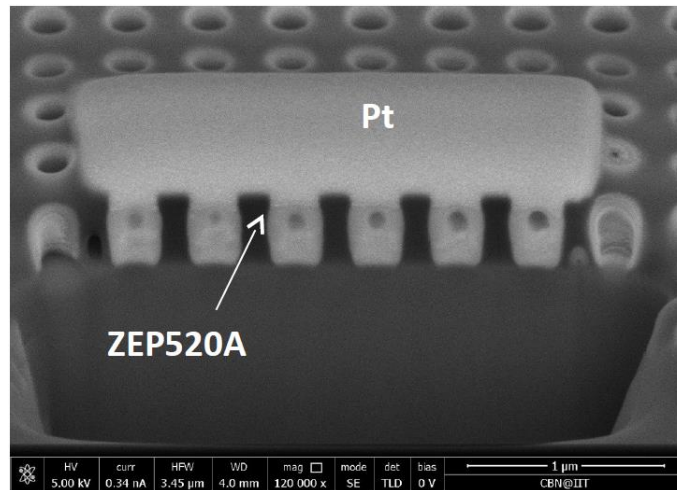
Figure 3.6: SEM cross section showing the complete development of the resist after 45s in xylene (the platinum has been deposited to protect the structure during the FIB cross section).

The main parameter in the development process has been the time, but it has been important taking into account others aspects:

- <u>the dose used for the EBL</u>: increasing the area dose, the time needed for a complete development became shorter because the weaker (for positive resist) or stronger (for negative resist) bindings between the molecules in the impressed areas;

- <u>the temperature of the solution:</u> like in any else chemical process, the temperature works as catalyst. So, higher is the temperature faster is the development;

- <u>agitation of the solution:</u> this aspect plays an important role when geometries with small features (like holes in the case of photonic crystals) are present. In this case a gently agitation has promoted the constant exchange of reagents on the sample, enhancing the developing.

3.4 Etching processes

The etching processes are techniques used to remove material from a layer or a substrate by means of chemicals dissolved in solution (**wet etching**) or in mixture of gases (**dry etching**). In both categories, there are some relevant parameters for designing and controlling the process:

- **Etching rate**: is the quantity of material removed (usually expressed by the thickness) per unit of time.

- **Directionality**: an etching process can be isotropic or anisotropic. In the first case the etching rate is the same in all directions, in the second one there is a direction for which the rate is higher than the others. In the case of wet or dry chemical etching, this parameter is mainly determined by the crystallographic directions of the material.

- **Selectivity**: it represents the preference of an etching process to etch a material than another one and it is quantified as the ratio of their etching rate.

Even if they have some parameters in common, the wet and dry etching have different performances and are suitable for different processes. In this work the dry etching has been used to transfer the photonic crystal on the Si_3N_4 after the lithography using the patterned ZEP520A e-beam resist as mask. The wet etching, instead, has been used to remove the silicon under the photonic crystal to get a free standing structure.

3.4.1 Inductively coupled plasma etching (ICP)

After the developing, the ZEP520A e-beam resist has been used as mask for the ICP etching in the transferring of the pattern on the Si_3N_4 layer, obtaining high resolution pattern and vertical side-walls. These performances have been possible by

tuning separately the chemical etching and the ion etching by means of two different RF generators. The system used in this work is the Oxford PlasmaPro Estrelas100 ICP (Figure 3.7).

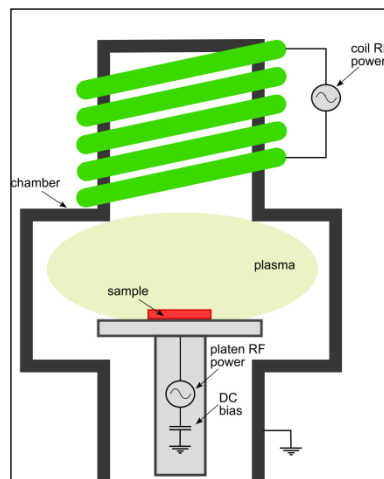**Figure 3.7:** ICP system at the IIT-CBN in Lecce (Italy).

Figure 3.8: Schematic of an ICP system.

As shown in Figure 3.8, the sample holder is connected to a RF generator (called **platen**) and is kept to a constant temperature using a flux of helium. The platen has the task to set the DC bias voltage on the holder determining the amount of ions etching. In contrast with the reactive ion etching (RIE) system, plasma is generated by a metal coil wrapped around the chamber and connected to a second RF generator (called **coil**). Changing the voltage of the coil it is possible to vary the plasma density and the concentration of the chemical reagents. The significant benefit introduced by the tuning of the two etching mechanism separately it is in the possibility to have dense plasma at low pressure. In this condition the mean-path of the ions is increased achieving a better anisotropicity and a higher etch-rate than the traditional RIE process.

For the etching of the Si_3N_4 a mixture of SF_6 and CHF_3 has been used and all the parameters have been opportunely tuned in order to obtain vertical sidewalls and uniform holes:

- SF_6: 20 sccm
- CHF_3: 80 sccm
- Pressure: 8 mTorr
- HF power : 75 W
- ICP power: 1500 W
- time: 1 min 05 sec

As it is possible to see in Figure 3.9, a fine optimization of the process has permitted to obtain sidewall angle of 86°C and a pattern reproducing the geometrical design parameters.
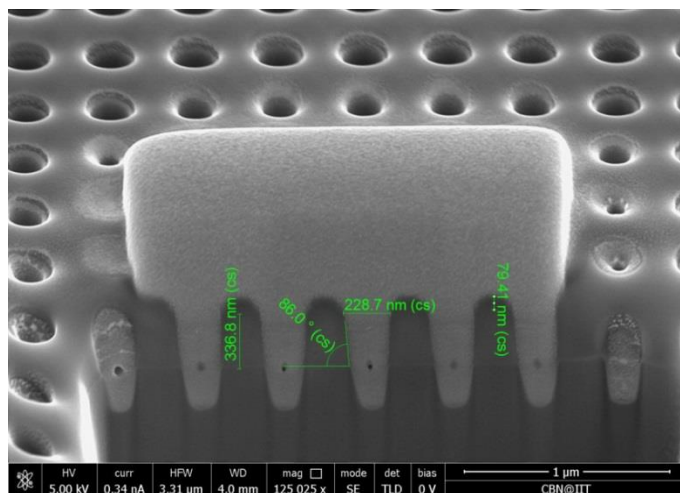
Figure 3.9: SEM cross-section of the structure after the ICP etching. (The platinum (Pt) has been deposited to protect the structure during the FIB cross section).

3.4.2 Wet etching

The last step of the process is the wet etching for the releasing of the membranes. This is a crucial step in the fabrication protocol that has to be finely optimized to obtain a good throughput.

The mechanism occurring during a wet etching consists in three steps, like shown in Figure 3.10: the reagents are carried for diffusion on the surface of the material that has to be removed and they bind with its molecules; then, the reaction products diffuse in the solution. More rapid and frequent this cycle is, higher is the etching rate. In particular, it is possible to detect some parameters affecting the etch-rate:

- The **concentration of reagents** in solution determines the amount of reaction per unit of time and then the etch-rate.

- The **temperature of solution** works as a catalyst so the increasing of the temperature increases the number of reactions in the unit of time and the etch-rate.

- The **agitation of the solution** increases the number of reagents that diffuse and leave the material. This aspect is important for structures

with high aspect ratio, like the etching of material with deep holes or trenches where the exchange of reagents is usually difficult.
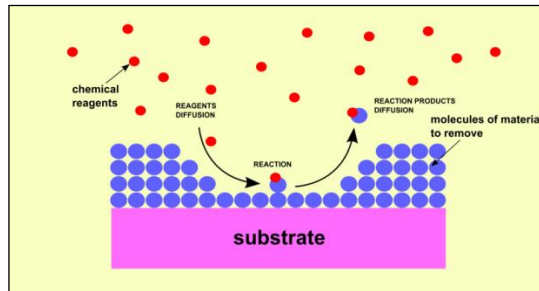
Figure 3.10: Mechanism occurring during a wet etching for the removal of material.

The wet etching has been performed in a TMAH based solution using the following recipe:

- ~2% TMAH in water solution
- Time: 30 minutes
- Temperature: 55°C
- Stirring: NO

which allowed us to achieve a free standing membrane (Figure 3.11) as reported in paper I.
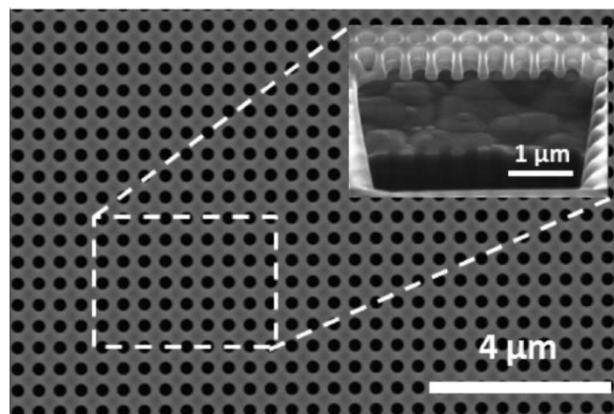
Figure 3.11: In plane SEM image and FIB cross section (inset) of the PhC membrane after the wet etching.

3.5 Summary

In this chapter the fabrication protocol has been illustrated, examining each step and the parameters to tune it. A PhC structure in membrane configuration has been realized with period p = 460 nm, radius r = 0.25*p and thickness t = 300 nm achieving high resolution and reproducibility. In the next chapter, the PhC membrane will be functionalized with a layer of antibodies for the recognition of the interleukin-6 protein and the immunosensor will be experimentally tested. Moreover, a further optimization of the fabrication process will be presented for the fabrication of PhC membrane for biosensing applications.

<div align="right">

Chapter 4

Proof of concept of a label-free immunosensor and further fabrication steps

</div>

4.1 Introduction

In the last chapter the fabrication protocol of the 2-D PhC membrane has been explained, highlighting the important parameters of each step. In this chapter, it is presented a proof-of-concept of the immunosensor, functionalizing the device with antibodies for the revelation of the interleukin-6 (IL-6) biomarker and performing some experimental tests of detection in solution. In the last part of the chapter some further steps about the fabrication of PhC membranes will be presented, in particular regarding the realization of complete suspended membranes and the transferring of structure on polymeric flexible material.

4.2 Experimental results

The optical characterization of the fabricated devices has been made enlightening the sample with a normal incidence light and collecting the reflected radiation by means of an optical multimode fiber (Figure 4.1).
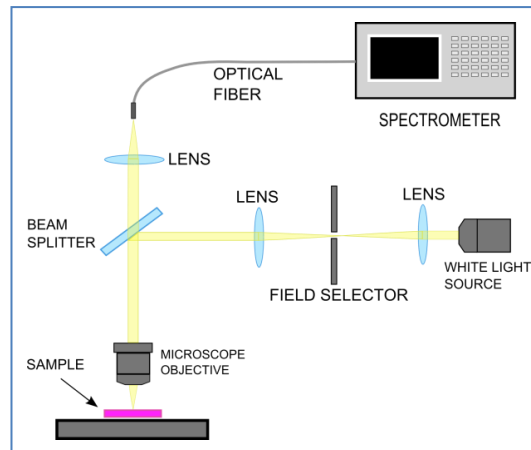
Figure 4.1: Set-up of measurement used to test the immunosensor (set-up of the NanoPhotonics and Electromagnetics Group, Politecnico di Bari).

In Figure 4.2 it is reported the comparison between the experimental and the simulated reflectivity spectrum in a IPA (n~ 1.3829) solution: as in the simulated data (blue line), the devices (red dotted line) presents two peaks, one in the VIS range (~ 640 nm) and the other one in the NIR range (~ 760 nm) showing correspondence between the theory and the experiments. To verify the capability in the sensing of refractive index variations, the spectrum has been experimentally measured in IPA, ethanol and in a mixture of both, showing a red shift of peak (Figure 4.3), as shown in paper II.

Figure 4.2: Comparison between the simulated (blue solid line) and the experimental (red dotted line) data of a PhC sensor with p = 460 nm r = 0.25*p immersed in IPA.

29

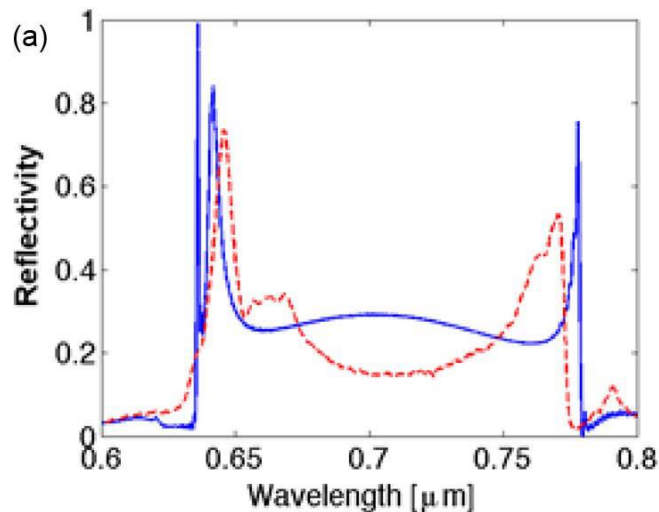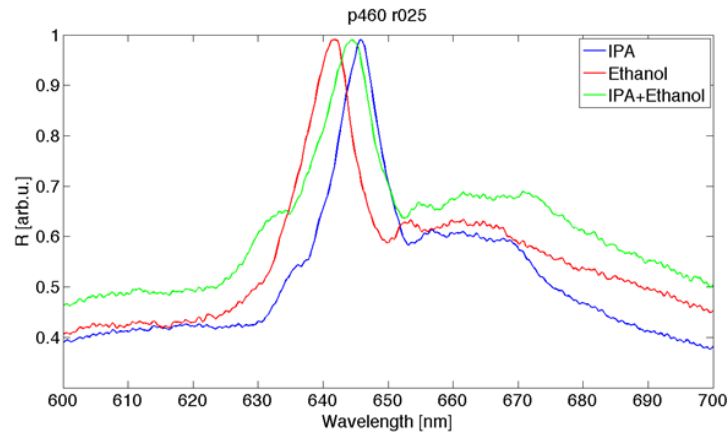**Figure 4.3:** Preliminary experimental results of the resonant peak shift in IPA, ethanol
(n~ 1.3616) and a combination of both.

After the preliminary measurements, the sensor has been functionalized
for the bio-selective detection of the IL-6[23], as shown in paper III. This step has
been performed at the Mawson Institute (University of South Australia).
Although the concentration of the IL-6 it is already measured by means of the
enzyme-linked immunosorbent assay (ELISA)[44], the process need time and
laboratory facility to be performed. The procedure consisted in the growing of a
layer of polymer on the surface and in the holes of the sensor by plasma
polymerization of the allyl glycidyl ether monomer. The thickness of the
deposited layer has been controlled varying the time of the process and after
some tests it has been chosen to fix it at 60 nm, as good compromise between the
not closing of the holes and the adequate density of the epoxy groups. After the
polymerization, the sensor has been measured again, showing a further red shift
due to the presence of this additional layer (Figure 4.4a). This has permitted to
verify the polymer homogeneity, checking the position of the peak in different
point on the PhC. Finally, the antibodies has been fixed on by means of the
reaction of their amine groups with the epoxy groups at a moderate alkaline pH
(100 g/ml antibody solution in 0.05 M carbonate buffer, pH 9.6), producing a

further peak shift. Remaining epoxide groups were blocked by 30 minutes incubation in 1 M ethanolamine solution.

In Figure 4.4b, it is reported the calibration curve obtained after consecutive IL-6 incubations. The sensitivity calculated on the initial slope is $2.1 \cdot 10^{-3}$ nm/(pg/ml) while the detection limit, calculated as 3σ/sensitivity (with σ standard deviation for the PBS solution without IL-6) is 1.5 pg/ml. Considering that the concentration of the IL-6 in a ill patient exceed 1 pg/ml[24], we can say that the limit of detection of the device is adequate to be employed as platform for immunosensing.
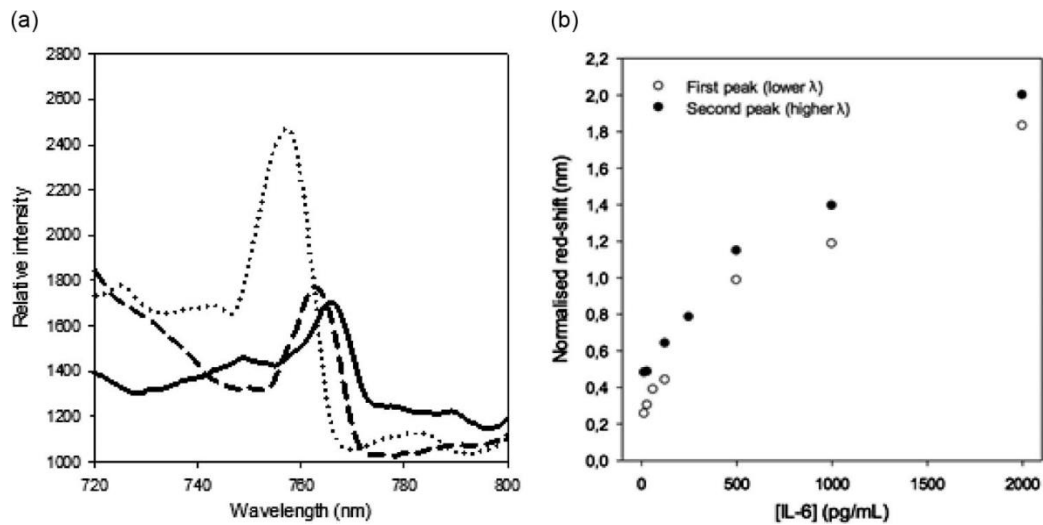
Figure 4.4: a) Measurements in PBS solution of the shift of the second peak of the structure during the functionalization process: prior the functionalization (dotted line), after the polymer deposition (dashed line) and after the antibodies immobilization (solid line). b) Calibration curve of the sensor after consecutive IL-6 incubation: the black and white dots represent the shift of the first and second peak for different IL-6 concentration.

In the next paragraph will be presented further steps in order to improve the performances of the fabricated membranes for biosensing applications. More in detail, two fabrication protocols will be described in order to achieve completely free standing membrane aiming to the transferring of both:

PhC biosensors on a tip of an optical fiber to realize biosensors for in-vivo detection of proteins concentration;

PhC membrane sensors on a polymeric flexible material, thus opening the way to a new generation of nanofabricated devices characterized by high resolution, integration and biocompatibility.

4.3 Further steps in the membranes fabrication for biosensing applications

The research activities carried out at the Photonics Group at the University of York dealt with the optimization of membranes fabrication protocol for biosensing applications. In the next paragraphs an optimized fabrication process for the realization of complete PhC free standing membranes and some preliminary results in the transferring of PhC membranes from a rigid substrate to a flexible layer will be presented. The processes have been optimized using the same wafer used for the fabrication of the immunosensor while in this case the structure is not more a pattern of 10×10 small membranes but a unique one $1mm^2$ area PhC membrane.

4.3.1 Fabrication process for complete free standing PhC membranes

A process for the fabrication of complete free standing PhC membranes has been studied and optimized. In Figure 4.5 is reported the first fabrication protocol developed at the University of York. We started the processing by opening a window of 1 mm $\times$ 1 mm on the backside Si_3N_4 by means of e-beam writing and reactive ion etching (RIE) etching. Then the Si has been removed by means of a wet etching using a potassium hydroxide (KOH) based solution (H_2O : KOH = 30 ml : 20 g, temperature 80°C and stirring at 300 rpm). In order to make the membranes robust enough to the fabrication of the PhC on the other side of the sample, the Si has not been completely removed, but a thin layer has been leaved under the Si_3N_4 layer (Figure 4.5 step 3).
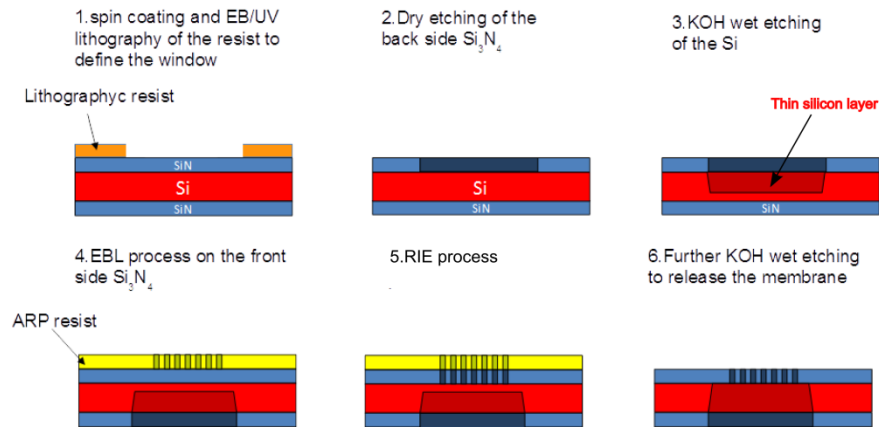
Figure 4.5: First version of the fabrication protocol used to achieve a complete free-standing membrane. A thin layer of silicon has been used to sustain the S₃iN₄ membrane during the fabrication process of the PhC.

The complete removal of the Si caused two problems. The first one was related to the deposition of the e-beam resist by spin coating used in the EBL for writing the PhC structure (step 4). In fact, the deposition resulted not uniform on the membrane, probably due to the bowing of the structure under the resist layer. The second one was caused by the large area of the membranes which was damaged during the RIE process (step 5). A way to make more robust the membranes and to obtain a more uniform resist deposition has been to block the KOH etching before to completely remove the Si, leaving a thin layer to sustain the membrane[45] in the next steps. After that, the sample has been processed on the other side in order to fabricate the PhC pattern. The geometrical parameters of the structure are the same used for the PhC immunosensor ($p = 460$ nm and $r = 0.25^*p$), but in this case it was composed by a unique 1 mm $\times$ 1 mm area PhC membrane and not by a matrix of smaller membranes as previously reported in Figure 3.3. A layer of AR-P 6200 has been deposited on the sample by spin-coating (with a spin speed of 2000 rpm for 60s and post bake for 10 minutes at 180°C) and exposed by means of RAITH VOYAGER™ (Figure 4.6) system with acceleration voltage of 50 kV, area dose of 130 μC/cm². The development has been done in xylene for 2 minutes as reported in Figure 4.5 at the step 4. Then, the PhC pattern has been transferred into the Si₃N₄ layer using a RIE (Figure 4.7)

process based on the following recipe:

- CHF$_3$: 58 sccm

- O$_2$: 2 sccm

- Pressure: 93 mTorr

- Potenza: 360 W

- Time preconditioning: 3 minutes

- Time: 17 minutes.

Figure 4.6: RAITH VOYAGER^{TM} system at the Photonic Group facilities (University of York (UK)).

Figure 4.7: RIE system at the Photonic Group facilities (University of York (UK)).

Finally, the remaining Si layer has been removed with a wet etching in KOH solution. In this step the residual stress of the Si_3N_4 layer has brought all the fabricated membranes to bend upward like cantilever and to break.

To overcome this issue the size of the membranes and of the PhC patterned on them have been varied in order to find a configuration not influenced by the residual stress. The membrane size has been reduced to 300 μm × 300 μm and it has been patterned with a PhC structure with dimensions 1 mm × 1 mm. In Figure 4.8 it is reported the new protocol where it is highlighted the absence of the thin Si layer after the KOH etching (step 3) and the last KOH etching at the step 6 while all the other steps are unchanged. In this way, it is not more necessary to leave the sustaining Si layer under the Si_3N_4 which is a critical step making more complex the fabrication protocol. Moreover, it is not suitable for samples containing more than one membrane, because of the not perfect uniformity of the etching on all the structures at the same time. Finally, the fabricated membranes are enough small to not suffer of the not uniformity of the resist deposition and to not be destroyed during the dry etching. The Figure 4.9 shows the complete structure where an area of 300 μm × 300 μm (included in the red dashed line) of the entire 1 mm x 1 mm PhC (included in the green dashed line) has been released by removing the Si underneath.
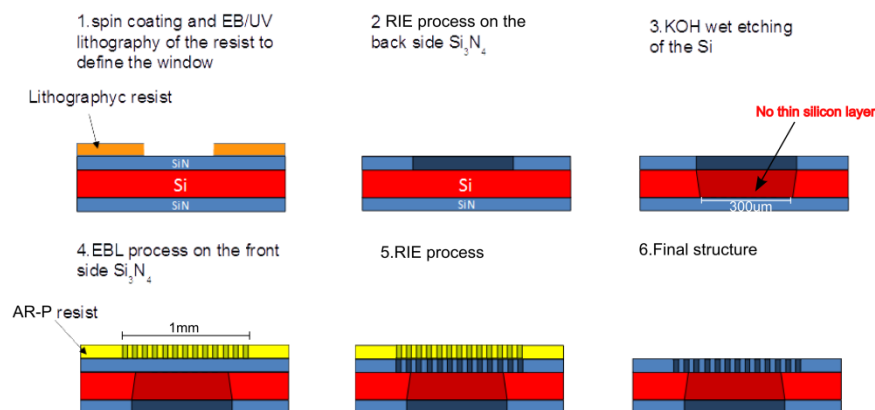

Figure 4.8: Final fabrication process for the fabrication of complete free-standing membrane. In this case the thin silicon layer is no more used (step 3) avoiding the last KOH etching (Figure 4.5 step 6).
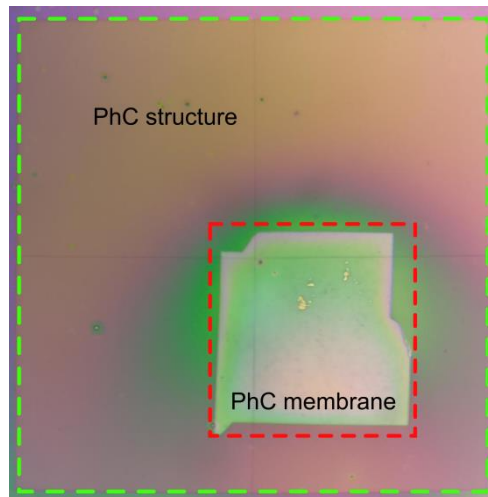
Figure 4.9: Image of a free standing membrane acquired by means of optical microscope where the green dashed line encloses the entire PhC structure, while the red dashed line contains the PhC membrane.

After the fabrication the structure has been inserted in a microfluidic system (Figure 4.10) and measured in reflectivity to check the presence of resonant peaks. The measurements performed in air have revealed the presence of a peak around 700 nm (Figure 4.11). A further measurement has been done in methanol (n ~1.32) showing a shift of the peak at around 750 nm.

Figure 4.10: Microfluidic system used to test the PhC membrane. The channel has been made in polydimethylsiloxane (PDMS) and placed on a microscope glass slice. Then, it has been covered with a transparent plastic sheet where the inlet and outlet have been obtained. The pipes have been connected to the system by means of two small pieces of PDMS fixed on the plastic sheet using epoxy glue.
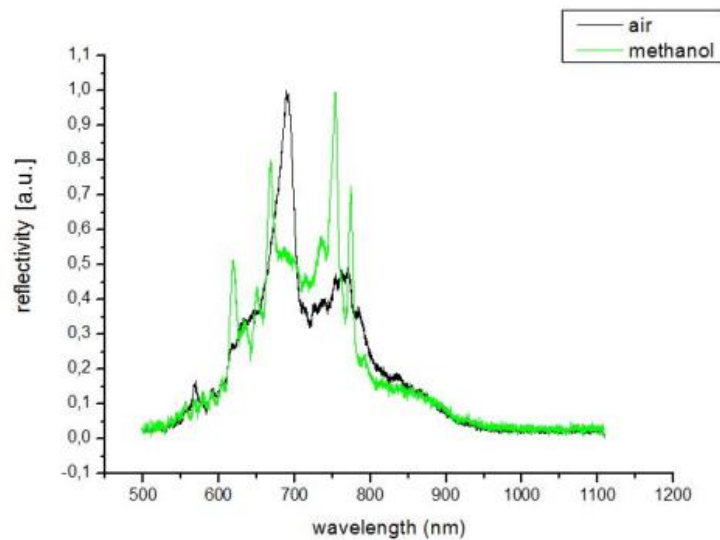
Figure 4.11: Reflectivity spectrum for the PhC membrane measured in air and methanol (n∼1.32).

A further step of this activity will be the transferring of the membrane on the tip of an optical fiber in order to realize biosensors for in-vivo detection of proteins concentration. A possible application of this device could be the detection of the dystrophin protein in patients affected by Duchenne muscular dystrophy disease, a genetic pathology arising in early age. Dystrophin is a protein contained in muscles with the task to sustain the cells membrane during the muscular contractions. The lack of this protein lead to the damaging of the cellular structure causing muscular dystrophy. For these reasons, the use of a non-invasive biosensor allowing in-vivo assays in muscles could be a fundamental aid to monitor the progress of the disease and to check the efficacy of medical treatments.

4.3.2 Preliminary testing in the substrate transferring

A further step in the fabrication of the immunosensor has been the study of a method to transfer it from a rigid substrate (Si in this case) to a polymeric flexible one, with the aim to improve the integrability and biocompatibility for

in-vivo assays.

The steps of the fabrication protocol are the following (Figure 4.12): a layer of AR-P 6200 resist has been spun on the layer of Si_3N_4 with a spin-speed of 2000 rpm for 60 s and post baked at a temperature of 180°C for 10 minutes. The resist has been patterned with an EBL process with voltage of 50 kV and area dose of 130 μC/cm² and developed in xylene for 2 minutes. The transfer of the PhC patterning on the Si_3N_4 layer has been achieved by RIE using the following recipe:

- CHF_3: 58 sccm
- O_2 : 2 sccm
- Pressure: 93 mTorr
- Potenza: 360 W
- Preconditioning time: 3 minutes
- Time: 17 minutes

Finally the membrane has been release using a dry etching in a solution of deionized water with the 3% of TMAH concentration for 15 minutes at 100°C. In Figure 4.13 is reported a picture of the 1 mm × 1 mm PhC membrane acquired by optical microscope. The darker colour in the centre of the membrane is caused by the absence of Si underneath and by means of this colour variation it is possible to check the progress of the wet etching (Figure 4.12 step 3) during the membrane releasing. Finally, the two lines passing in the middle of the structure are due to the stitching error, that is the mismatching between the write-fields during the EBL process.
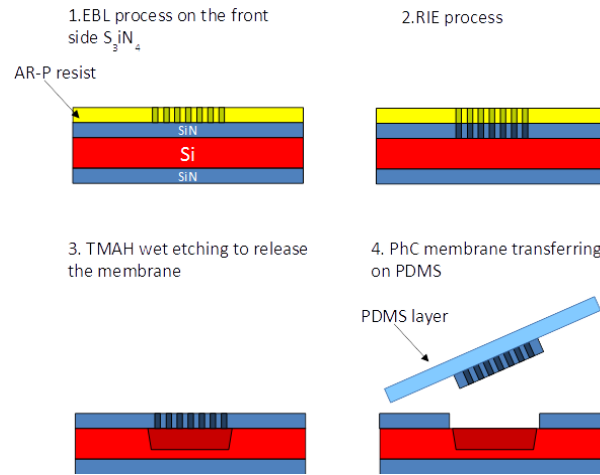
Figure 4.12: Fabrication process for the transferring of the PhC membrane on flexible substrate.
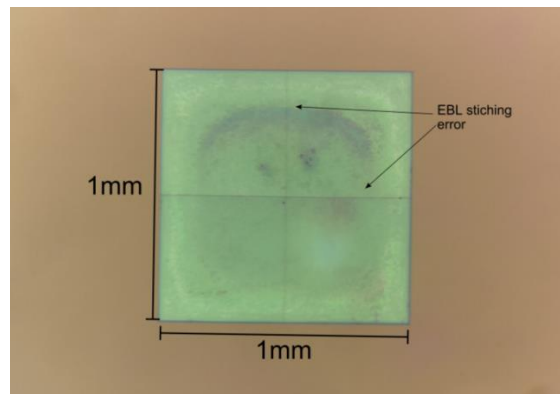
Figure 4.13: Image acquired by optical microscope of the PhC 1 mm × 1 mm membrane after the wet etching in TMAH solution. The colour variation in the centre of the structure represents the absence of Si underneath while the lines passing in the middle are caused by the EBL stitching error.

Then the sensor has been transferred on a thin layer of polydimethylsiloxane (PDMS n ~ 1.4) using the process described by M.G. Scullion et al.[46]. The PDMS has been prepared by mixing 5 ml of silicon elastomer with 0.5 ml of curing agent and degassed. After that, a thin layer (less than 1 mm) has been deposited in a plastic box and has been left in oven at 60°C for several hours. At this point, the sample has been pressed on the PDMS and then peeled off, leaving the membrane attached on the polymer (Figure 4.14). The transferred structure has been measured revealing a peak of reflectivity around 750 nm (Figure 4.15).
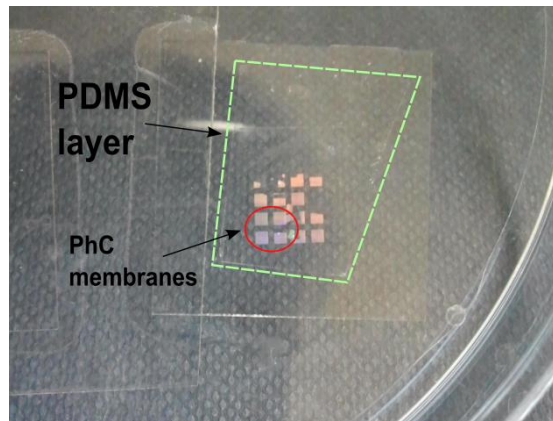
Figure 4.14: Picture of an experimental test about the transferring of PhC structures on PDMS. The sample is placed on a microscope coverslip. The little fragments between the larger structures are pieces of membranes detached during the TMAH etching (Figure 4.19 step 3). The complete membrane transferred has an area of 1 mm × 1 mm. The process needs further optimizations to increase the number of complete transferred structures.
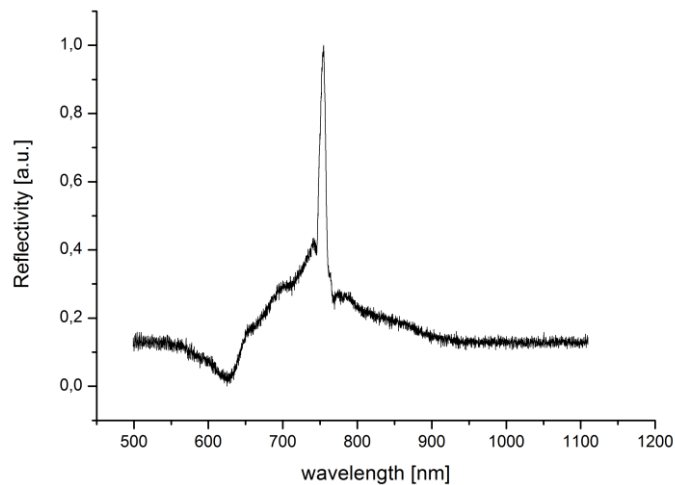
Figure 4.15: Reflectivity spectrum of the PhC (p = 460 nm r = 0.25*p) on PDMS measured in air.

A further step of this activity will be the design of a new PhC structure to be transferred on PDMS, optimizing its electromagnetic properties for biosensing applications and opening the way to a new generation of nanofabricated devices characterized by high resolution, integration and biocompatibility.

4.4 Summary

In this chapter has been presented the proof-of-concept of a label-free immunosensor for the revelation of biomarkers in solution. Initially, the reflectivity spectrum of the sensor has been tested in different refractive index solutions, showing a diverse shift of the reflection peak wavelength in each one. Subsequently, it has been functionalized with a layer of antibodies for the revelation of the IL-6 biomarker, building the calibration curve and determining a limit of detection of 1.5 pg/ml, quite below the concentration of the protein in a ill patient.

In the last part of the chapter the activity carried out at the Photonics Group of the University of York has been discussed. It has been studied the fabrication process to achieve completely free standing membrane for an innovative procedure for the transferring of PhC biosensors on a tip of an optical fiber to realize biosensors for in-vivo detection of proteins concentration. Finally, some experimental tests are illustrated about the optimization of the process for the transferring of PhC membrane sensors on a polymeric flexible material.

Conclusion

The aim of this thesis has been the design, fabrication and testing of a label-free immunosensor for the revelation of biomarkers in solution. The project has been a collaboration between the IIT-CBN centre, Politecnico di Bari and the Mawson Institute (University of South Australia).

To get the goal, a 2-D photonic crystal (PhC) slab with square lattice has been designed by means of numerical simulation using the finite difference time domain (FDTD) method. The structure consists in a 1 mm × 1 mm area Si_3N_4 with thickness of 300 nm. The geometrical parameters like lattice period and radius has been optimized getting reflectivity peaks around 640 nm and 760 nm.

The designed structure has been fabricated by means of a nano-fabrication protocol composed by e-beam lithography, dry and wet etching. Each step has been optimized achieving high quality membranes with high reproducibility as it has been proved by morphological characterization by means of scanning electron microscopy.

The PhC membrane has been functionalized by means of a layer of antibodies for the revelation of the interleukin-6 protein, a biomarker in relation with diseases like oral cancer and Alzheimer. The immunosensor has been tested in the revelation of the protein in solution, building a calibration curve. The detection limit determined from the tests has been of 1.5 pg/ml, a lower quantity than the usual concentration of the protein in ill patients.

In the last part of the activities (carried out at the Photonics Group of the University of York (UK)) further optimizations of the fabrication protocol of PhC membranes for biosensing applications have been proposed. In particular, a complete free standing PhC membrane with area 300 μm × 300 μm has been obtained, which will be used in the process for the transferring of biosensors on a tip of an optical fiber to realize biosensors for in-vivo detection of proteins concentration.

Finally, some tests about the transferring of 1 mm × 1 mm PhC

membranes from rigid substrate to polymeric layers have been performed, procedure that will be optimized for the realization of high resolution and biocompatibility biosensors.

References

[1] J. Castillo, S. Gáspár, S. Leth, M. Niculescu, A. Mortari, I. Bontidean, V. Soukharev, S. A. Dorneanu, A. D. Ryabov, and E. Csöregi, "Biosensors for life quality," *Sensors Actuators B Chem.*, vol. 102, no. 2, pp. 179–194, 2004.

[2] T. Vo-Dinh and B. Cullum, "Biosensors and biochips: advances in biological and medical diagnostics," *Fresenius. J. Anal. Chem.*, vol. 366, no. 6–7, pp. 540–551, 2000.

[3] R. Monošík, M. Streďanský, and E. Šturdík, "Biosensors - classification, characterization and new trends," *Acta Chim. Slovaca*, vol. 5, no. 1, pp. 109–120, 2012.

[4] S. P. Mohanty and E. Kougianos, "Biosensors: A tutorial review," *IEEE Potentials*, vol. 25, no. 2, pp. 35–40, 2006.

[5] P. B. Luppa, L. J. Sokoll, and D. W. Chan, "Immunosensors—principles and applications to clinical chemistry," *Clin. Chim. Acta*, vol. 314, no. 1–2, pp. 1–26, 2001.

[6] S. M. Borisov and O. S. Wolfbeis, "Optical Biosensors," *Chem. Rev.*, vol. 108, no. 2, pp. 423–461, 2008.

[7] P. J. Conroy, S. Hearty, P. Leonard, and R. J. O'Kennedy, "Antibody production, design and use for biosensor-based applications," *Semin. Cell Dev. Biol.*, vol. 20, no. 1, pp. 10–26, 2009.

[8] R. Mayeux, "Biomarkers: potential uses and limitations," *NeuroRx*, vol. 1, no. 2, pp. 182–188, 2004.

[9] S. Naylor, "Biomarkers: current perspectives and future prospects," *Expert Rev. Mol. Diagn.*, vol. 3, no. 5, pp. 525–529, 2003.

[10] X. Fan, I. M. White, S. I. Shopova, H. Zhu, J. D. Suter, and Y. Sun, "Sensitive optical biosensors for unlabeled targets: A review," *Anal. Chim. Acta*, vol. 620, no. 1–2, pp. 8–26, 2008.

[11] T.-Y. Chang, M. Huang, A. A. Yanik, H.-Y. Tsai, P. Shi, S. Aksu, M. F. Yanik, and H. Altug, "Large-scale plasmonic microarrays for label-free

high-throughput screening," *Lab Chip*, vol. 11, no. 21, pp. 3596–3602, 2011.

[12] S. K. Dondapati, T. K. Sau, C. Hrelescu, T. A. Klar, F. D. Stefani, and J. Feldmann, "Label-free biosensing based on single gold nanostars as plasmonic transducers," *ACS Nano*, vol. 4, no. 11, pp. 6318–6322, 2010.

[13] M. Grande, M. A. Vincenti, T. Stomeo, G. Morea, R. Marani, V. Marrocco, V. Petruzzelli, A. D'Orazio, R. Cingolani, M. De Vittorio, D. de Ceglia, and M. Scalora, "Experimental demonstration of a novel bio-sensing platform via plasmonic band gap formation in gold nano-patch arrays," *Opt. Express*, vol. 19, no. 22, pp. 21385–21395, 2011.

[14] H. J. Lee, J. H. Lee, H. S. Moon, I. S. Jang, J. S. Choi, J. G. Yook, and H. Il Jung, "A planar split-ring resonator-based microwave biosensor for label-free detection of biomolecules," *Sensors Actuators, B Chem.*, vol. 169, pp. 26–31, 2012.

[15] T. Claes, J. G. Molera, K. De Vos, E. Schacht, R. Baets, and P. Bienstman, "Label-free biosensing with a slot-waveguide-based ring resonator in silicon on insulator," *IEEE Photonics J.*, vol. 1, no. 3, pp. 197–204, 2009.

[16] N. Skivesen, A. Têtu, M. Kristensen, J. Kjems, L. H. Frandsen, and P. I. Borel, "Photonic-crystal waveguide biosensor," *Opt. Express*, vol. 15, no. 6, pp. 3169–3176, 2007.

[17] A. M. Armani, R. P. Kulkarni, S. E. Fraser, R. C. Flagan, and K. J. Vahala, "Label-Free, Single-Molecule Detection with Optical Microcavities," *Science*, vol. 317, no. 5839, pp. 783–787, 2007.

[18] L. Martiradonna, F. Pisanello, T. Stomeo, A. Qualtieri, G. Vecchio, S. Sabella, R. Cingolani, M. De Vittorio, and P. P. Pompa, "Spectral tagging by integrated photonic crystal resonators for highly sensitive and parallel detection in biochips," *Appl. Phys. Lett.*, vol. 96, no. 11, p. 113702, 2010.

[19] M. R. Lee and P. M. Fauchet, "Two-dimensional silicon photonic crystal based biosensing platform for protein detection," *Opt. Express*, vol. 15, no.

8, pp. 4530–4535, 2007.

[20]   D. Dorfner, T. Zabel, T. Hürlimann, N. Hauke, L. Frandsen, U. Rant, G. Abstreiter, and J. Finley, "Photonic crystal nanostructures for optical biosensing applications," *Biosens. Bioelectron.*, vol. 24, no. 12, pp. 3688–3692, 2009.

[21]   F. Pisanello, M. De Vittorio, and R. Cingolani, "Modal selective tuning in a photonic crystal cavity," *Superlattices Microstruct.*, vol. 47, no. 1, pp. 34–38, 2010.

[22]   T. Kishimoto, "The Biology of Interleukin-6," *Blood*, vol. 74, no. 1, pp. 1–10, 1989.

[23]   J. M. Fernandez-Real, M. Vayreda, C. Richart, C. Gutierrez, M. Broch, J. Vendrell, and W. Ricart, "Circulating interleukin 6 levels, blood pressure, and insulin sensitivity in apparently healthy men and women," *J. Clin. Endocrinol. Metab.*, vol. 86, no. 3, pp. 1154–9, 2001.

[24]   F. Riedel, I. Zaiss, D. Herzog, K. Götte, R. Naim, and K. Hörmann, "Serum levels of interleukin-6 in patients with primary head and neck squamous cell carcinoma," *Anticancer Res.*, vol. 25, no. 4, pp. 2761–2766, 2005.

[25]   E. Yablonovitch, "Inhibited Spontaneous Emission in Solid-State Physics and Electronics," *Phys. Rev. Lett.*, vol. 58, no. 20, pp. 2059–2062, 1987.

[26]   S. John, "Strong localization of photons in certain disordered dielectric superlattices," *Phys. Rev. Lett.*, vol. 58, no. 23, pp. 2486–2489, 1987.

[27]   J. D. Joannopoulos, S. G. Johnson, J. N. Winn, and R. D. Meade, *Photonic Crystals: Molding the Flow of Light (Second Edition)*. Princeton University Press, 2011.

[28]   Lord Rayleigh, "XXVI. On the remarkable phenomenon of crystalline reflexion described by Prof. Stokes," *The London, Edinburgh, and Dublin Philosophical Magazine and Journal of Science*, vol. 26, no. 160. pp. 256–265, 1888.

[29]   M. El Beheiry, V. Liu, S. Fan, and O. Levi, "Sensitivity enhancement in

photonic crystal slab biosensors," *Opt. Express*, vol. 18, no. 22, pp. 22702–14, 2010.

[30]   S. G. Johnson, S. Fan, P. R. Villeneuve, J. D. Joannopoulos, and L. A. Kolodziejski, "Guided modes in photonic crystal slabs," *Phys. Rev. B*, vol. 60, no. 8, pp. 5751–5758, 1999.

[31]   S. Fan and J. D. Joannopoulos, "Analysis of guided resonances in photonic crystal slabs," *Phys. Rev. B*, vol. 65, no. 23, p. 235112, 2002.

[32]   W. Zhou, D. Zhao, Y. C. Shuai, H. Yang, S. Chuwongin, A. Chadha, J. H. Seo, K. X. Wang, V. Liu, Z. Ma, and S. Fan, "Progress in 2D photonic crystal Fano resonance photonics," *Prog. Quantum Electron.*, vol. 38, no. 1, pp. 1–74, 2014.

[33]   "Meep" [Online]. Available: http://ab-initio.mit.edu/wiki/index.php/Meep.

[34]   K. S. Yee, "Numerical solution of initial boundary value problems involving Maxwell's equations in isotropic media," *IEEE Trans. Antennas Propag*, vol. 14, no. 3, pp. 302–307, 1966.

[35]   J.-P. Berenger, "A Perfectly Matched Layer for the Absorption of Electromagnetic Waves," *J. Comput. Phys.*, vol. 114, no. 2, pp. 185–200, 1994.

[36]   C. Vieu, F. Carcenac, A. Pepin, Y. Chen, M. Mejias, A. Lebib, L. Manin-Ferlazzo, L. Couraud, and H. Launois, "Electron beam lithography: resolution limits and applications," *Appl. Surf. Sci.*, vol. 164, no. 1, pp. 111–117, 2000.

[37]   T. Stomeo, A. Passaseo, R. Cingolani, and M. De Vittorio, "Fast nanopatterning of two-dimensional photonic crystals by electron beam lithography," *Superlattices Microstruct.*, vol. 36, no. 1–3, pp. 265–270, 2004.

[38]   M. De Vittorio, M. T. Todaro, T. Stomeo, R. Cingolani, D. Cojoc, and E. Di Fabrizio, "Two-dimensional photonic crystal waveguide obtained by e-beam direct writing of SU8-2000 photoresist," *Microelectron. Eng.*, vol. 73–

74, pp. 388–391, 2004.

[39] A. van de Kraats and R. Murali, "Proximity effect in electron beam lithography," Atlanta, Georgia: Nanotechnology Research Center, Georgia Institute of Technoogy, 2005.

[40] M. Parikh, "Corrections to proximity effects in electron beam lithograhy. I. Theory," *J. Appl. Phys.*, vol. 50, no. 6, pp. 4371–4377, 1979.

[41] G. Owen and P. Rissman, "Proximity effect correction for electron beam lithography by equalization of background dose," *J. Appl. Phys.*, vol. 54, no. 6, pp. 3573–3581, 1983.

[42] S. Lee and B. D. Cook, "PYRAMID — A Hierarchical , Rule-Based Approach Toward Proximity Effect Correction — Part II: Correction," vol. 11, no. 1, pp. 108–116, 1998.

[43] A. Gangnaik, Y. M. Georgiev, B. McCarthy, N. Petkov, V. Djara, and J. D. Holmes, "Characterisation of a novel electron beam lithography resist, SML and its comparison to PMMA and ZEP resists," *Microelectron. Eng.*, vol. 123, pp. 126–130, 2014.

[44] A. Voller, A. Bartlett, and D. E. Bidwell, "Enzyme immunoassays with special reference to ELISA techniques," *J. Clin. Pathol.*, vol. 31, no. 6, pp. 507–520, 1978.

[45] C. Nicholaou, "Improving the detection Limit of Planar 2D Photonic Crystal Slab Refractive Index Sensors," University of Toronto, 2013.

[46] M. Scullion, M. Fischer, and T. Krauss, "Fibre Coupled Photonic Crystal Cavity Arrays on Transparent Substrates for Spatially Resolved Sensing," *Photonics*, vol. 1, no. 4, pp. 412–420, 2014.